Synthesis and Characterization of Poly(ferrocenylsilanes) with Coumarin Side Groups and Their Photochemical Reactivity and Electrochemical Behavior

ARTICLE *in* MACROMOLECULES · MAY 2007

Impact Factor: 5.8 · DOI: 10.1021/ma062502o

5 AUTHORS, INCLUDING:

Biye Ren
South China University of Technology
58 PUBLICATIONS **808** CITATIONS
SEE PROFILE

Zhen Tong
South China University of Technology
197 PUBLICATIONS **3,743** CITATIONS
SEE PROFILE

Synthesis and Characterization of Poly(ferrocenylsilanes) with Coumarin Side Groups and Their Photochemical Reactivity and Electrochemical Behavior

Biye Ren,* Dongli Zhao, Shanshan Liu, Xingxing Liu, and Zhen Tong*

Research Institute of Materials Science, South China University of Technology, Guangzhou 510640, China

Received October 29, 2006; Revised Manuscript Received March 13, 2007

ABSTRACT: Two novel photoreversible poly(ferrocenylsilanes) (PFS) with coumarin side groups, i.e., half- and whole-substituted poly(ferrocenyl(3-(7-hydroxycoumarin) propyl)methylsilane), are synthesized by transition metal-catalyzed ring-opening polymerization of ferrocenyl(3-chloropropyl) methylsilane monomer and subsequent group exchange and nucleophilic substitution reaction. The two polymers are characterized by elemental analysis, ^{1}H and ^{13}C NMR, FTIR, UV−vis, emission spectra, TG, and DSC. Their photochemical reactivity and electrochemical behavior are studied by UV−vis spectra and cyclic voltammetry, respectively. The two PFS polymers, like coumarin derivatives, can undergo reversible photodimerization and photoscission, but the content of coumarin significantly affects their photochemical reactivity and electrochemical properties. The photochemical reaction of coumarin side groups can cause a reversible change of electrochemical behavior of these PFS polymers, i.e., the peak separation ΔE increases with photodimerization and decreases with photoscission again. Cyclic voltammograms indicate that the electrode processes of the films of both original and photo-cross-linked polymers coated on a glassy carbon electrode are diffusion controlled and quasireversible in a wide scan rate range in 0.1 M NaCl aqueous solution at room temperature because of a low rate of mass diffusion and slow rate of the change transfer between the active sites, judged from small kinetic parameters such as surface transfer coefficient αn_α, standard rate constant K_s, and apparent diffusion coefficient D_{app} of the electroactive species. Interestingly, the electrode process of the half-/whole-substituted PFS polymer was less reversible than the half-substituted one at high scan rate. Photoirradiation causes the electrode processes of the two coumarin PFS polymers to become less reversible due to the cross-linking of the films. These coumarin PFS polymers may have potential use in many fields because they combine the useful photochemical reactivity with redox activity.

Introduction

Organometallic polymers have received considerable attention in the past decade in light of their uses as chemical sensors, electrocatalysts, modified electrodes, and photoelectronic devices.[1,2] Since the discovery of high-molecular-weight poly(ferrocenylsilanes) **(**PFS**)** ($M_n > 10^5$) through a thermal ring-opening polymerization (ROP) route from strained cyclic, silicon-bridged [1]ferrocenophane precursors in the early 1990s,[3] a wide range of PFS polymers (homopolymers and copolymers) with various interesting physicochemical properties have been subsequently synthesized from analogous strained monomers containing other bridging elements (germanium, tin, phosphorus, sulfur, etc.) and transition metals or different π-hydrocarbon rings.[4] Living anionic ROP and transition metal catalyzed ROP routes of silicon-bridged [1]ferrocenophanes have also been established for the synthesis of well-defined organometallic block copolymers.[5] Among organometallic materials, the high-molecular-weight PFS polymers are of particular interest and represent one class of best studied organometallic polymers as a result of the interesting optical, unique electronic, magnetic, and exceptional thermal and chemical stability.[6] These PFS materials have shown exceptional potential for application in many fields such as semiconductors, sensors, optical crystals, etching resists, redox-active gels, liquid crystals, and nonlinear optical devices.[2−7]

In recent years, there has been a growing interest in the synthesis of new functional PFS polymers for special application in electric devices, electrocatalysis, and sensors.[2,4] It has shown that the substituents on a silicon atom significantly influence the physicochemical properties of PFS, which opens another opportunity to synthesize new PFS polymers by simply introducing the functional side groups into a silicon atom.[4] A conventional route to functional PFS materials is to utilize functional silicon-bridged [1]ferrocenophanes monomers. For example, Tang et al.,[8] recently synthesized a series of novel PFS polymers using functional silicon-bridged [1]ferrocenophanes with different electron-rich substituents on silicon by thermal ROP. These novel PFS polymers can form charge-transfer complexes with iodine and tetracyanoethylene (TCNE) to produce interesting electrochemical and magnetic properties dependent on substituents on silicon. Another convenient approach to the functionalization of PFS is postpolymerization functionalization with reactive groups on PFS such as hydrosilyl, chlorosilyl, haloalkylsilyl, and aminoalkyl groups[4,9] because the introduction of a wide range of small functional molecules can endow the PFS polymer precursor with some special structures and properties without synthesizing new silicon-bridged [1]-ferrocenophanes. For example, Liu et al.,[10] recently reported the synthesis and thermal properties of calamitic thermotropic side chain liquid-crystalline PFS via hydrosilylation of poly(ferrocenylmethylhydrosilane) with ethylene monomers. A variety of hydrophilic and water-soluble neutral and cationic high-molecular-weight PFS have been also reported via nucleophilic substitution reactions of the chlorosilyl group on PFS.[9] Among PFS polymers with a haloalkylsilyl group, such as poly(ferrocenyl(3-chloropropyl)methylsilane) (**1**), may be a more attractive route to the incorporation of functional groups into

* Corresponding authors. E-mail: mcbyren@scut.edu.cn (B.R.); mcztong@scut.edu.cn (Z.T.). Fax: (86)-20-87110273.

10.1021/ma062502o CCC: $37.00
Published on Web 05/26/2007

Scheme 1

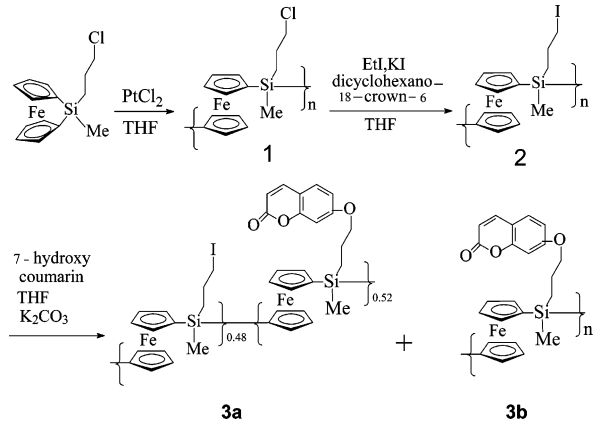

the PFS side chain,[11] because polymer **1** is usually very stable and can be readily synthesized by transition metal catalyzed ROP of the corresponding (3-chloropropyl)methylsilyl[1]-ferrocenophane and converted quantitatively into its bromopropyl or iodopropyl analogues via a halogen exchange reaction. A variety of PFS polymers can be obtained by means of nucleophilic substitution reactions of the corresponding bromopropyl or iodopropyl analogues of polymer **1**. Hempenius et al.,[12] synthesized several water-soluble poly(ferrocenylsilane) polyelectrolytes. These new main-chain organometallic polyelectrolytes have been utilized by layer-by-layer technology to fabricate the super thin electroactive films,[13] which have potential application in electrode modification, electrocatalysis, electrochromism, and nano- and microlithographic applications.

The PFS materials with photoresponsive moieties may be an interesting and attractive field from a scientific viewpoint. Recently, Manners et al.[14] first reported the synthesis of a photo-cross-linkable PFS, which have potential use as an etching resist. On the other hand, polymers with coumarin moieties are very useful in many fields, such as laser dyes, photoresists, energy-transfer materials, and alignment agents for liquid crystals, because of the photodimerization ability of the coumarin unit through the [2−2] cyclization of the double bond.[15] The introduction of photoreversible moieties onto silicon as a side chain of PFS would render some promising properties of these materials. Also, the thermal stability and mechanical properties of these PFS polymers can be enhanced through photo-cross-linking. However, to our knowledge, little study on the photoreversible PFS polymers has been reported up to data. More recently, we[16] reported a brief communication on the photochemical and electrochemical properties of a novel photoreversible PFS with coumarin side groups by the incorporation of 7-hydroxycoumarin into a PFS precursor with 3-iodopropyl group. It has been shown that this novel PFS polymer can undergo reversible photodimerization and photoscission, which further influence its electrochemical activity. This is a very interesting and useful phenomenon, which may endow these materials with some special applications for modified electrodes, electrochemical sensors, and nonlinear optical devices. It is therefore important to illustrate the effects of the content of coumarin moiety on their photochemical reactions, redox properties, electrode process, and charge transfer.

In this study, we build on the preliminary results presented in our recent letter to provide a more complete account of the synthesis and characterization of photoreversible PFS polymers **3a**−**b** (Scheme 1**)** with different contents of coumarin moiety at silicon atom. In particular, we focus on the effect of photodimerization and photoscission reactions of coumarin moieties on their physicochemical, especially electrochemical behavior, which will be helpful in understanding the redox properties of these novel functional PFS materials, the mechanism of the electrode process, and the factors that affect charge transfer.

Experimental Section

Materials. Ferrocene, dichloro(3-chloropropyl)methylsilane, *n*-butyllithium, iodoethane, potassium iodide, 7-hydroxycoumarin, dicyclohexano-18-crown-6, and $PtCl_2$ were purchased from Aldrich and used as received. *N*,*N*,*N*′,*N*′-Tetramethyldiamine (TMEDA) was purified by refluxing with sodium and redistilled before use. All of the solvents were dried over Na−K alloy and distilled under an argon atmosphere before use. All reaction and manipulation were carried out under an atmosphere of high pure argon using Schlenk techniques and in a glove box filled with high pure argon. Dilithioferrocene−TMEDA were synthesized according to the same method reported by Manners et al.[3] Polymer precursors **1** and **2**, and also the (3-chloropropyl)methylsilyl ferrocenophane monomer, were synthesized using procedures previously described in the literature and include the proper reference.[11−13]

Measurements. NMR spectra were recorded on Bruker Avance 400 in $CDCl_3$ or C_6D_6. Thermogravimetric analysis (TG) and differential scanning calorimetry (DSC) were measured using a Netzsch DSC 204 at a heating/cooling rate of 10 °C/min under nitrogen. Molecular weights were determined by gel permeation chromatography (GPC) with a Waters apparatus at 40 °C using THF as solution and narrowly distributed polystyrene as standard. Fourier transform infrared (FTIR) spectra were measured with a Bruker Vector 33 on carefully dried samples embedded in KBr pellets. Fluorescence emission spectra were measured with a Hitachi F-4500 fluorescence spectrophotometer, with the excitation and emission slits of 5 nm at 25 °C and the excitation wavelength 320 nm. UV spectra were measured on a Hitachi U-3010 spectrophotometer.

The photodimerization reaction of polymer dissolved in THF (2.8×10^{-4} M) in an air-proof quartz cell was carried out at room temperature by irradiation of a 450 W high-pressure mercury lamp at the wavelength exceeding 300 nm for up to 180 min. The cross-linked samples were irradiated at 254 nm UV with a low-pressure mercury lamp for photocleavage reaction.

The cyclic voltammetry (CV) measurements were carried out under argon in solution of 0.1 M NaCl using a CHI 750A electrochemical workstation (CHI Instruments, Shanghai). The PFS-coated glassy carbon electrode was used as the working electrode with an Ag/AgCl (3 M KCl) reference electrode and a platinum wire counter electrode. As a general procedure, first a Teflon-shrouded glassy carbon rockered electrode (diameter $\phi = 3$ mm, geometric area $s = 0.071$ cm^2) was polished to a mirror finish with 0.05 μm Al_2O_3 paste on 0.6 μm sandpaper, cleaned by ultrasonication in double-distilled water and successively in anhydrous ethyl alcohol twice, and then dried for further electrochemical measurements. For preparation of the PFS-coated electrode, a THF solution of polymer was used to cover the glassy carbon disk electrodes and then dried sufficiently and slowly at room temperature to make compacted films. The photodimerization and photoscission reactions of the polymer films coated on a glassy carbon electrode were carried out according to the above same procedure.

Synthesis of Polymer 3a. To a solution of polymer **2** (1.2 g, 3.03 mmol repeat units) in 30 mL of THF, 7-hydroxycoumarin (0.294 g, 1.81 mmol) and anhydrous potassium carbonate (0.23 g, 1.81 mmol) were added and stirred for 3 days. Then 15 mL of this solution was taken out and precipitated into 300 mL of hexane, dried in vacuum to get a yellow polymer **3a** (0.49 g). GPC (THF): $M_n = 9.89 \times 10^4$ g/mol, $M_w = 1.91 \times 10^5$ g/mol, $M_w/M_n = 1.93$. ^{1}H NMR ($CDCl_3$) δ: 0.41 (s, CH_3), 0.98 (m, Si−CH_2), 1.87 (m, CH_2), 3.18 (t, CH_2−I), 4.0 (t, −CH_2−O−), 3.94−4.21 (m, Cp rings), 6.19−7.59 (coumarin). ^{13}C NMR ($CDCl_3$) δ: −3.1 (CH_3), 12.1 and 12.4 (Si−CH_2), 18.5 and 23.9(CH_2), 28.9 (CH_2−I), 71.1 (−CH_2−O−), 70.1−77.3 (Cp rings), 101.3−162.4 (coumarin).

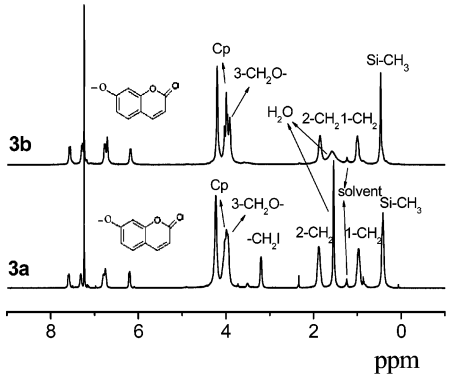

Figure 1. ^{1}H NMR spectra (400 MHz) and the assignments of **3** in $CDCl_3$.

$(C_{14}H_{17}IFeSi)_{0.48}-(C_{23}H_{22}O_3Si)_{0.52}$: calcd, C 53.25, H 4.75; found, C 53.28, H 4.94.

Synthesis of Polymer 3b. 7-Hydroxycoumarin (0.36 g, 2.2 mmol) in 10 mL of THF and 0.3 g of anhydrous potassium carbonate were added into the solution of polymer **2** (1.2 g, 3.03 mmol repeat units) in 30 mL of THF and stirred for 6 days, then poured into 300 mL hexane and dried in vacuum to obtain a yellow polymer **3b** (0.53 g, 70%). GPC (THF): $M_n = 1.00 \times 10^5$ g/mol, $M_w = 1.97 \times 10^5$ g/mol, $M_w/M_n = 1.96$. ^{1}H NMR ($CDCl_3$): δ = 0.47 (s, CH_3), 0.99 (m, Si−CH_2), 1.85 (m, CH_2), 4.0 (t, −CH_2−O−), 3.94−4.21 (m, Cp rings), 6.19−7.59 (coumarin). ^{13}C NMR ($CDCl_3$) δ: −3.2 (CH_3), 12.4 (Si−CH_2), 23.9 (CH_2), 71.1 (CH_2−O−), 70.1−77.3 (Cp rings), 101.3−162.4 (coumarin). $C_{23}H_{22}O_3Si$ (430.36): calcd, C 63.32 H 5.15; found, C 62.43 H 5.25.

Results and Discussion

1. Synthesis and Characterization of Polymers 3. The synthetic route of PFS with coumarin side groups is represented in Scheme 1. The polymers **1**−**3** were characterized by GPC, elemental analysis, FTIR, UV−vis, and ^{1}H and ^{13}C NMR. Figure 1 shows the 400 MHz ^{1}H NMR spectra and the assignments of polymers **3a** and **3b** in $CDCl_3$. We can see that polymer **3a** has the resonance signal at 3.18 ppm caused by 3-CH_2I, while the signal at 3.18 ppm (3-CH_2I) shifts to 4.0 ppm (3-CH_2O−) in the ^{1}H NMR spectra of **3b**, indicative of the complete conversion of **2** into **3b** via macromolecular nucleophilic substitution reaction.[11] The UV−vis spectra of the polymers in THF are shown in Figure 2A. Both **3a** and **3b** show two main absorptions at 237 and 320 nm. The former results from the $\pi-\pi^*$ electron transition of ferrocenyl (Fc) unites in polymer main chains, and the latter is attributed to the maximum absorption of coumarin moieties. The maximum emissions λ_{em} of **3a** and **3b** in THF appears at 371 nm (Figure 2B), which slightly blue-shifts about 12 nm compared to λ_{em} = 383 nm of free 7-oxycoumarin in THF. The incorporation of 7-oxycoumarin moiety into the PFS precursor **2** is also confirmed by the FTIR, as showed in Figure 3. Both **3a** and **3b** exhibit the absorptions of C═C rings at 1626, 1555, 1509, and 1468 cm^{-1} and the stretch absorptions of C═O group at 1733 cm^{-1} and asymmetric C−O−C bond at 1121 cm^{-1}, which correspond to the characteristic absorption bands of coumarin moiety, also polymers **2** and **3a** have the stretch vibration absorption of C−I at 488 cm^{-1}, which disappears in FTIR of **3b**. It is clear that the coumarin moiety is successfully introduced into the PFS side chain by macromolecular nucleophilic substitution reaction.

2. Thermal Properties. It was well-known that the substituents on silicon significantly influenced the thermal property of PFS polymers.[4] The thermal behavior of polymers **3** was characterized using TG and DSC. The measured results are shown in Table 1. No significant weight loss is observed below 280 °C for polymers **3**, indicative of a higher thermal stability. The degradation temperature T_d corresponding to the maximum weight-loss rate is 288 and 301 °C for **3a** and **3b**, respectively. **3b** has slightly higher T_d value than **3a**, indicating that the coumarin side group has a slightly positive influence on the thermal stability of PFS polymers, but not distinctive. Furthermore, as reported by Manner et al.[17] previously, side residues

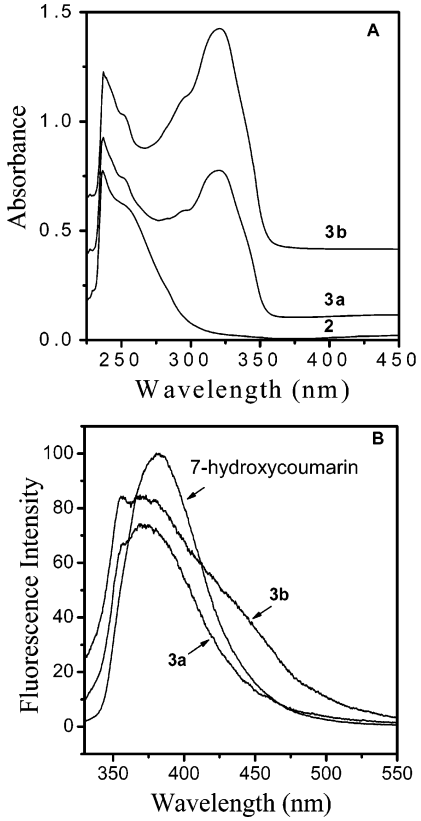

Figure 2. UV−vis spectra (A) of polymers **2** and **3** in THF. Emission spectra (B) of **3** and 7-hydroxycoumarin in THF.

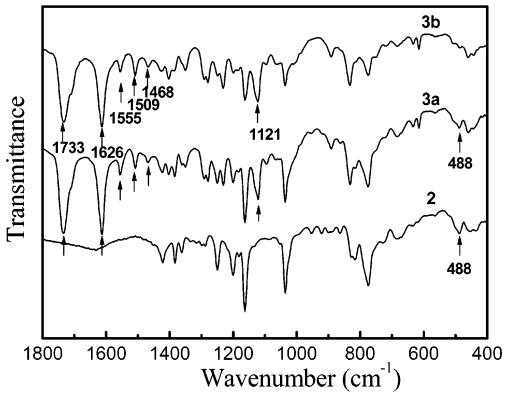

Figure 3. FTIR spectra of polymers **2** and **3**. The curves are vertically shifted to avoid overlapping.

Table 1. GPC Measured Results and Thermal Properties of Polymer 3

polymers	M_n (× 10^4)	M_w (× 10^4)	PDI (M_w/M_n)	T_g (°C)	T_d (°C)
2	9.2	18.0	1.92	42	285
3a	9.8	19.1	1.93	66	288
3b	10.0	19.7	1.97	76	301
3a* [a]				76	312
3b* [a]				80	350

[a] Cross-linked samples after irradiation for 180 min.

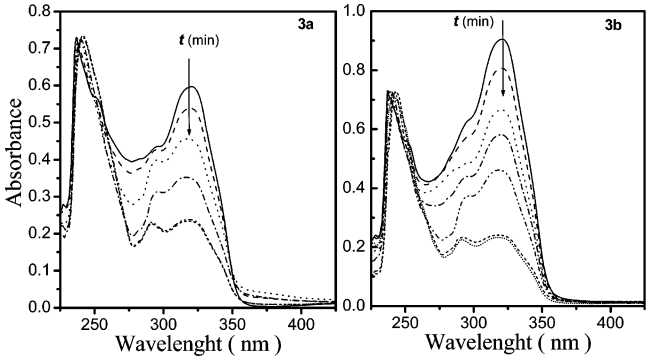

Figure 4. UV−vis spectra of **3a** (left) and **3b** (right) in THF (2.8×10^{-4} g/mL) against irradiation time *t* with a 450 W high-pressure Hg lamp.

can strongly influence the T_g values of PFS polymers, for example, the T_g values of poly(ferrocenyldiakylsilanes) possessing a methyl or ethyl substituent are about 33 and 22 °C, respectively. DSC curves indicate that there is a clear glass transition for polymers **3**, but no melting transition is observed over the temperature from −60 °C up to decomposition temperature, indicating an amorphous structure of **3** due to asymmetric substituents of coumarin moiety on silicon because symmetric substituents on PFS usually favor crystallization, while asymmetrically substituted PFS polymers are usually amorphous.[17] The measured T_g values are 66 and 76 °C for **3a** and **3b**, which are respectively 24 and 35 °C higher than the corresponding precursor **2**. The higher T_g values for polymer **3** should be attributed to the bulky coumarin side groups, which effectively reduces the mobility of polymer chains. Therefore, the whole-substituted **3b** has higher T_g than the corresponding half-substituted **3a** as a result of a higher coumarin content in **3b**.

3. Photochemical Reactivity of Coumarin Side Groups. As we know, coumarin and its derivatives can undergo reversible photodimerization and photoscission reactions when irradiated with different UV wavelength.[15] The photodimerization of **3** is successfully performed through the dimerization addition of coumarin with a 450 W high-pressure Hg lamp. As shown in Figure 4, before photoirradiation, polymer **3b** exhibits a main absorption peak at 320 nm from the maximum absorption of coumarin moieties. Its absorbance at 320 nm (A_{320}) significantly deceases with prolonging the photoirradiation time *t*, resulting from the dimerization of the coumarin groups. The coumarin chromophore is known to undergo only [2+2] photodimerization because of its fused-ring structure.[18] As the coumarin dimerizes, the level of unsaturation decreases due to the formation of cross-links of the coumarin side groups via [2+2] photodimerization.[19] Therefore, the decrease in A_{320} can be primarily attributed to the loss of coumarin chromophores as a result of UV-light-induced photodimerization. The photodimerization of polymers **3** is further verified by TG and DSC measurements also. As may be seen from Table 1, the degradation temperature T_d of **3a** is raised from 288 to 312 °C, and also T_d of **3b** is greatly increased from 301 to 350 °C after irradiation for 180 min. The increase in T_d of **3** after irradiation should result from the photo-cross-linking. In addition, the photoirradiation causes **3** to exhibit a slightly higher T_g than the original **3** before irradiation. This implies that the mobility of the polymer chains is largely limited due to photo-cross-linking. As an illustration, the photoreaction process of polymer **3b** is denoted in Scheme 2.

On the basis of the above discussion, the change in A_{320} value directly reflects the degree of cross-linking of polymers **3**, hence

Scheme 2

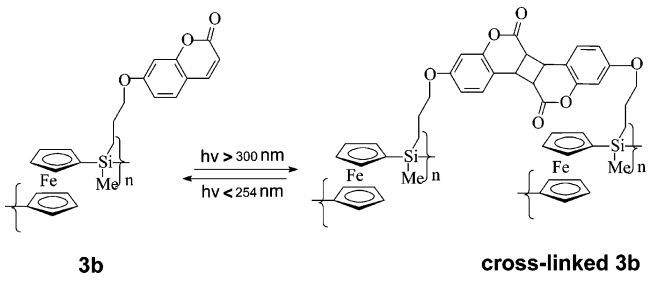

the cross-linking density of **3** can be approximately estimated from the A_{320} value using the following expression:

$$D = \frac{(A_{320})_0 - (A_{320})_t}{(A_{320})_0} \times 100\% \qquad (1)$$

where *D* is the degree of cross-linking, $(A_{320})_0$ and $(A_{320})_t$ are is the absorbance of polymers **3** at 320 nm before irradiation and after irradiation for *t* min, respectively. Figure 5 depicts the dependence of the A_{320} and *D* values of **3** on UV irradiation time *t*. It is also noted that the A_{320} is leveled off after irradiation for 150−180 min, indicating that the photodimerization reaction of **3b** seems to become more and more slow and difficult after irradiation for about 150 min. As for the half-substituted **3a**, UV−vis spectra exhibit a similar change trend with photoirradiation, but its A_{320} decreases more slowly than that of **3a**, suggesting that the higher coumarin content attached to polymer main chains, the faster the photodimerization reaction occurs. The higher T_d of the photo-cross-linked **3b** suggests that **3b** should have a higher cross-linking density than **3a** after 150−10 min of photoirradiation. For an easy comparison, a plot of the *D* values against *t* is shown in Figure 5 also. The determined maximum cross-linking degree D_{max} is 60% and 75% for **3a** and **3b**, respectively. This indicates that the photodimerization reaction of **3** is incomplete regardless of the coumarin content in their structures and high coumarin content favors the photodimerization of coumarin side groups in polymer. A longer irradiation time or a higher exposure of irradiation may be necessary for complete photodimerization of coumarin side groups. In other words, the higher the coumarin content, the faster the rate of photodimerization and the higher the cross-linking density of the coumarin polymers. The present results suggest that the content of coumarin in polymers should be an important factor affecting their photodimerization reactions.

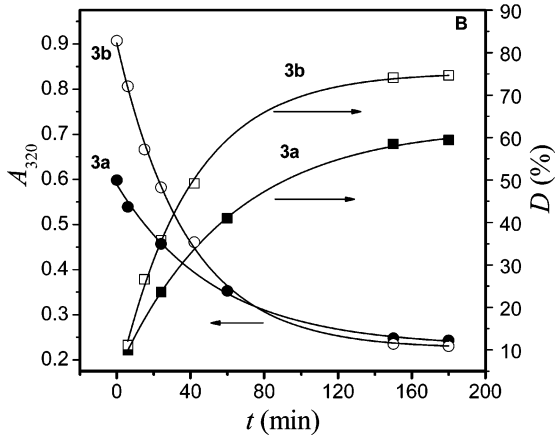

Figure 5. Plots of the absorbance (A_{320}) at 320 nm and cross-linking degree (*D*) of polymers **3** against the irradiation time *t* during photodimerization.

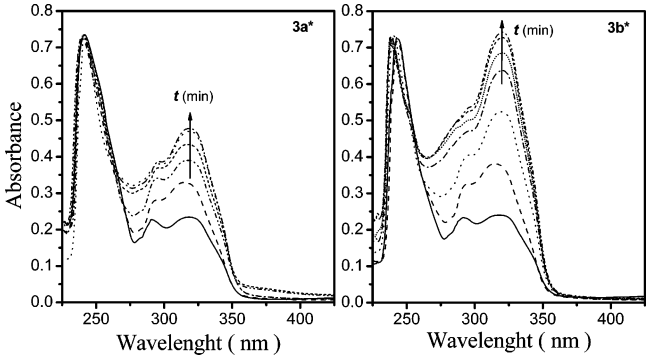

Figure 6. UV−vis spectra of the cross-linked **3a** and **3b** in THF (2.8 × 10^{-4} g/mL) against irradiation time *t* with a 254 nm low-pressure Hg lamp. Cross-linked samples are represented by *.

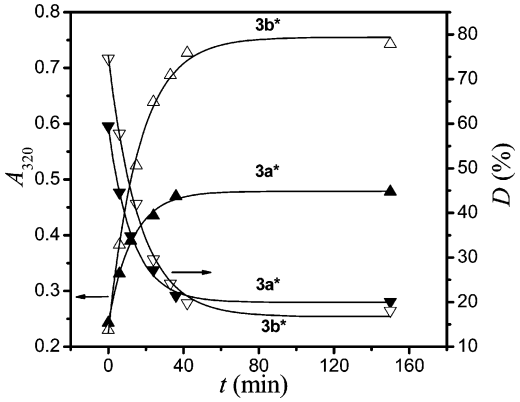

Figure 7. Plots of the absorbance (A_{320}) at 320 nm and cross-linking degree (*D*) of polymers **3** against the irradiation time *t* during photoscission reactions. Cross-linked samples are represented by *.

On the other hand, it was well-known that the cyclobutane ring in the photodimer of coumarin can be cleaved to regenerate coumarin by photoirradiation with short wavelength (<300 nm).[15] It is therefore interesting to make a comparative study on photoscission reactions of the two photo-cross-linked PFS polymers **3a** and **3b**, which are respectively termed as **3a*** and **3b*** (similarly hereinafter). As an illustration, Figure 6 shows UV−vis spectra of **3a*** and **3b*** after irradiation for different time *t* with a 254 nm wavelength. As expected, the A_{320} value of both **3a*** and **3b*** significantly increases with prolonging irradiation time, indicating that the cyclobutane ring in a photodimer of coumarin moiety is gradually cleaved to regenerate coumarin.[15] However, a leveling off in the absorbance is observed after irradiation for 150−180 min, which leads to a slight lower final absorbance than that of original polymers without irradiation, indicating an incomplete photocleavage of photoinduced cyclobutane. A plot of the A_{320} and *D* values of **3a*** and **3b*** versus UV irradiation time *t* is shown in Figure 7 for the photoscission process. It is found that the final cross-linking degree is respectively lowered to 20% and 18% for **3a*** and **3b*** after 180 min of photoirradiation, as may be easily seen from Figure 7. The photocleavage degree can be estimated by $D^* = (1 - D_t/D_0) \times 100\%$, where D^* is the photoscission degree; D_0 and D_t are the cross-linking degree when photoscission occurs for 0 and *t* min, respectively. It is found that the whole-substituted **3b*** has higher photoscission degree (76%) than the corresponding half-substituted **3a*** (66%), showing that only part of the photodimers can be reverted back to the starting material. This suggests that the higher coumarin content favors the photoscission reaction, which is similar to the results of photodimerization. It should be mentioned that in the film of **3** coated on a quartz glass can take place the same photochemical reactions as the solution of **3** and no significant difference is observed (not shown).

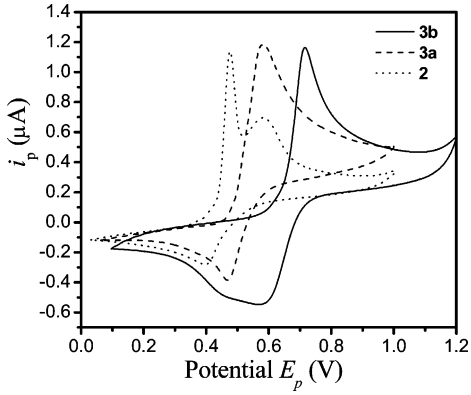

Figure 8. Cyclic voltammograms of the polymer films coated on a glassy carbon electrode at the scan rate of 10 mV/s in 0.1 M NaCl solution at 25 °C.

4. Electrochemical Behaviors of Polymers 3. Cyclic voltammetry (CV) is one of the most used tools to study electroactive polymers. These polymers are studied by CV in 0.1 M NaCl at 25 °C to illustrate the effects of coumarin content on the electrochemical behavior. To obtain stable and reproducible cyclic voltammograms, cyclic voltammograms of polymers coated on a GC electrode are recorded with successive potential sweeps from 0 to +1.2 V (vs SCE) at a scan rate of 10 mV/s until reaching a steady state, i.e., the voltammetric currents hardly show decrease and the peak separation keep constant with potential sweep. The CV curves of the films of polymers **3** are illustrated in Figure 8. The coverage degree Γ of the electrode is estimated to be 3.319 × 10^{-6} and 3.451 × 10^{-6} mol/cm^2 for **3a** and **3b**, respectively. For polymer **3a**, the CV curve shows a couple of redox peaks, and polymer **3b** shows one sharp oxidation peak and a wide reduction peak at a scan rate of 10 mV/s. Particularly, the potential peaks of polymer **3b** shift anodically compared with **3a**. This indicates that the electron-rich coumarin substituent onto the PFS side chain significantly affects the electrochemical behavior of these PFS polymers. The displacements in the peaks for the two polymers appears to be due to the electronic differences between the iodide and coumarin substituent or due to the difference in coumarin content because the bulky coumarin moiety may baffle the mobility of the Fc uniting in polymer chains and hinder the charge transfer and the diffusion of the electrolyte into the polymer films.

The above photochemical experiments have demonstrated that the coumarin side groups in polymers **3** can undergo photodimerization and photoscission reactions. It becomes of interest whether the photodimerization and photoscission reaction affect the electrochemical behaviors of PFS films or not. To illustrate this, the CV measurements of polymer-modified electrodes are carried out for photodimerization process at 25 °C. As an illustration, Figure 9 shows the cyclic voltammograms of polymer **3b** films after UV irradiation for different times. We can see that the oxidation potential E_{pa} of **3b** increases with the irradiation time *t* but the reduction potential E_{pc} of **3b** keeps almost stable or changes little; as a result, the peak separation ΔE increase with time *t*. The E_{pa} keep stable after 150−180 min of irradiation. This is consistent with the time that polymers **3** reach the maximum cross-linking degree during photodimerization process, as may be seen in Figure 5. Generally, the kinetic reversibility of the redox couple can be assessed

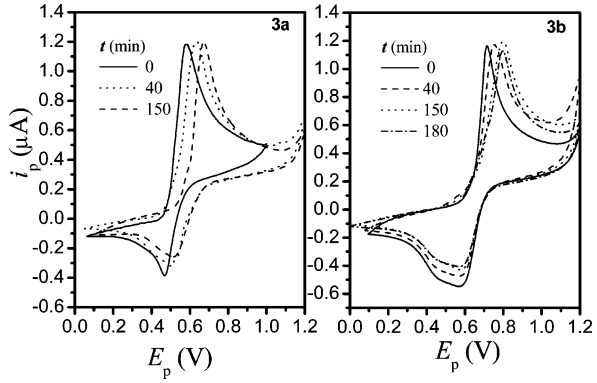

Figure 9. Cyclic voltammograms of the film of **3a** and **3b** coated on a glassy carbon electrode after irradiation for different time *t* with a 450 W high-pressure Hg lamp at the scan rate of 10 mV/s in 0.1 M NaCl solution at 25 °C.

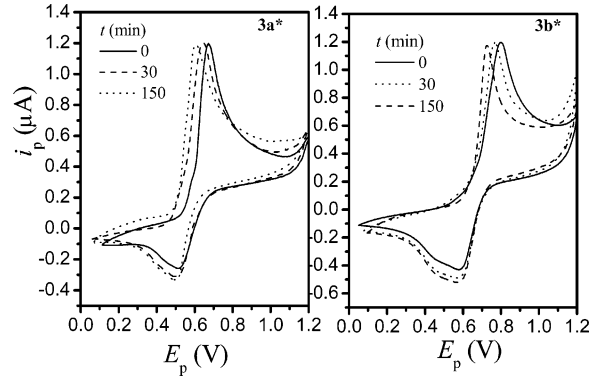

Figure 10. Cyclic voltammograms of the photo-cross-linked **3a** and **3b** films on a glassy carbon electrode after irradiation with a 254 nm UV light for different time *t* at the scan rate of 10 mV/s in 0.1 M NaCl solution at 25 °C. Cross-linked samples are represented by *.

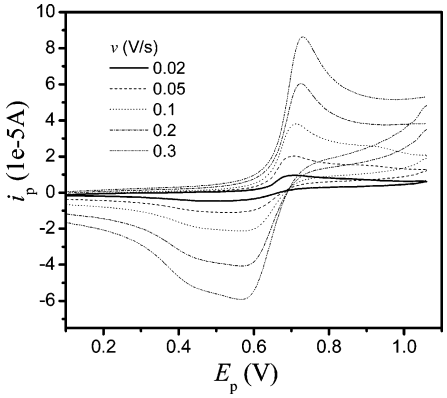

Figure 11. Cyclic voltammograms of the film of polymers **3b** coated on a glassy carbon electrode at different scan rate ranging from 0.02 to 0.3 V/s in 0.1 M NaCl solution at 25 °C.

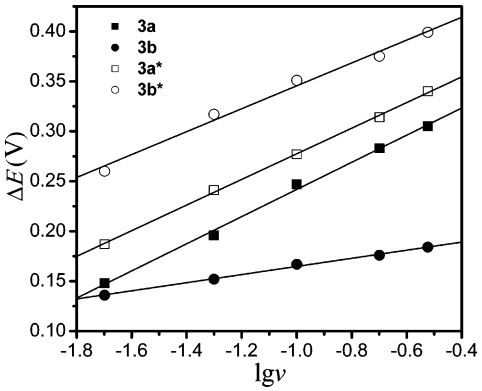

Figure 12. Plots of the peak separation Δ*E* of polymers **3** coated on a glassy carbon electrode against the logarithm log *v* of the scan rate at the scan rate range of 0.02−0.3 V/s in 0.1 M NaCl solution at 25 °C. Cross-linked samples are represented by *.

according to the separation of the anodic and cathodic peak potential in CV.[20] The increase of Δ*E* indicates that polymer **3b** becomes more and more difficult to oxidize and the reversibility of electrode process becomes less after UV irradiation because the mobility of the polymer chains is further restricted after photoirradiation due to the formation of photo-cross-linking structure in systems so that the resistivity of the film increases, the rate of mass diffusion decreases, and the charge transfer between the active sites becomes more and more difficult. But coumarin as an electron-rich group should favor the reduction process itself; hence, the E_{pc} of **3b** keeps almost stable. The similar change in CV is also observed for polymer **3a** after UV irradiation, but its photodimerization leads to a smaller maximum peak separation $\Delta E_{(max)}$ than **3b**. The $\Delta E_{(max)}$ value is 152 and 219 mV for **3a*** and **3b***, respectively, which is 38 and 85 mV larger than that of the corresponding original polymers **3a** and **3b**. The larger $\Delta E_{(max)}$ value of the cross-linked **3b** may be attributed to its denser film and larger resistivity resulting from higher cross-linking density. Furthermore, we also observe from Figure 11 that the oxidization peak current (i_{pa}) of polymers **3** keeps stable but the corresponding reduction peak current ($|i_{pc}|$) slightly decreases with the photodimerization reaction. The reason for this may be that the dimerization of coumarin moiety would slowly weakens its electron-donating power after photo-cross-linking. If the above discussion is reasonable, then the photoscission of the cross-linked polymers would have a contrast effect on the electrochemical behavior of films with photodimerization.

Figure 10 shows the CV curves of the photo-cross-linked **3** after irradiation for different times with shorter wavelength. As expected, the oxidation potential E_{pa} of both **3a*** and **3b*** gradually decreases with photoscission reaction of cyclobutane ring, and the reduction potential E_{pc} keeps almost stable or changes little, indicative of an almost reversible change of the redox behavior with the photoscission reaction. The E_{pa} of **3a*** and **3b*** reaches their minimum value after irradiation for 150−180 min. For example, the minimum E_{pa} of **3b*** is 730 mV after photoscission for 150 min, which is only slightly 10 mV larger than that of uncross-linked **3b** before irradiation. The small difference is consistent with the incomplete photocleavage of the cyclobutane ring in the cross-linking polymers. Moreover, in contrast to the photodimerization process, the $|i_{pc}|$ value increases during the process of photoscission because the regenerated electron-donating coumarin group favors to the reduction process.

5. Electrode Process Mechanism of Polymers 3. To further reveal the electrode process mechanism of the coumarin PFS films, the CV measurement is carried out at different scan rate in 25 °C. It is observed that the reduction peaks of the films of **3** shifts cathodically and the oxidation peaks shifts anodically as the scan rate increases. As a result, the peak separation Δ*E* increased with increasing scan rate. According to the electrochemical theory,[20] in a reversible electrode process, the peak potential *E* is independent of scan rate, while in a totally irreversible process, there is only an oxidation peak or a reduction one. We also study the variation of peak separations Δ*E* on scan rate. Figure 12 depicts a plot of Δ*E* against the logarithm of the scan rate. As seen, the Δ*E* linearly increases over the range of 20−300 mV/s for all polymer-modified electrodes, indicating that the electrode processes of the cou-

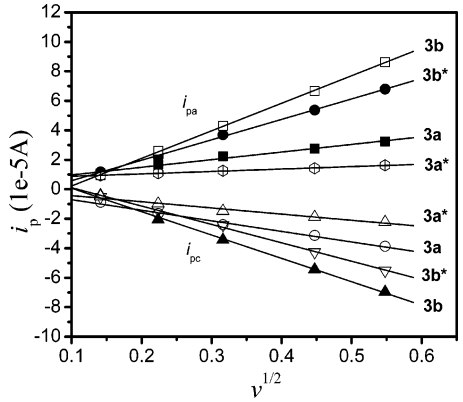

Figure 13. Plots of the peak current i_p of polymers **3** coated on a glassy carbon electrode against the square root $v^{1/2}$ of the scan rate at the scan rate range of 0.02−0.3 V/s in 0.1 M NaCl solution at 25 °C. Cross-linked samples are represented by *.

marin polymer-modified electrodes are quasireversible in the above scan rate range. Moreover, the redox peak current ($|i_p|$) of polymer films significantly increased with increasing scan rate from 20 to 300 V/s also, but the anodic current i_{pa} is always larger than the cationic current $|i_{pc}|$. As is known, for diffusion-controlled electrode processes, the peak current $|i_p|$ linearly increases with the square root of potential scan rate $v^{1/2}$. Figure 13 depicts a plot of i_p vs $v^{1/2}$ over the range of 20−300 mV/s. Good linear relationships between i_p and $v^{1/2}$ are also obtained in the above same scan range for all modified electrodes. Therefore, the CV measurements suggest that the electrode processes of the films of polymers **3** are diffusion controlled and quasireversible in the above scan rate range.[20] The linear regression equations obtained are shown in Table 2.

It was known that, for a diffusion-controlled electrode process of the surface-immobilized redox species, i_p and ΔE can be expressed as follows:[21]

$$i_p = 0.4958nF(\alpha n_\alpha)^{1/2}\left(\frac{F}{RT}\right)^{1/2} AD_0^{1/2}C_0^* v^{1/2} \quad (2)$$

$$i_p = 0.227nFAC_0^* k^0 \exp\left[-\left(\frac{\alpha n_\alpha F}{RT}\right)(E_p - E^{0'})\right] \quad (3)$$

$$\Delta E = (2.303RT/\alpha n_\alpha F)(\log(RTK_s/2.184\alpha n_\alpha FD_0) - \log v) \quad (4)$$

where i_p is the peak current in *A*, *A* is the area of film coverage of the electrode surface in cm^2, v is the potential scan rate in V/s, αn_α is the surface charge-transfer coefficient for the surface-immobilized redox species, K_s is the standard rate constant in cm/s, C_0^* is the concentration of the electroactive species in the films in mol/cm^3, D_0 is the apparent diffusion coefficient of the electroactive species in cm^2/s, and $E^{0'}$ is the apparent formal potential. From eqs 2−4, we can get three important kinetic parameters, αn_α, K_s, and D_0, which manifest the electrochemical behavior, electrode process mechanism, and charge transfer.

To calculate these kinetic parameters, αn_α, K_s, and D_0 here, we assume that the film thickness d is approximately 10 μm, then C_0^* is obtained by $C_0^* = \Gamma/d$ because the concentration of Fc uniting in the film is difficult to be measured accurately. The calculated $\alpha n_\alpha$and K_s and apparent diffusion coefficient D_{app} are listed in Table 2 also. As seen from Table 2, films of polymers **3** have small αn_α, D_{app}, and k_s values, indicating slow diffusion rates of the electroactive species, low electron exchange efficiency at the electrode surface, and low rate of charge transport between the films and the electrode. As a result, the electrode processes of the two polymer films are quasi-reversible over the range of 20 mV/s because these parameters, especially αn_α, are factors to reflect the electrode surface electron exchange efficiency or the reversibility of the electrode process.[20] It is worth noting that polymer **3b** has larger αn_α, K_s, and D_{app} values than **3a**. This means that the film of polymer **3b** allows a faster rate of charge transport and electron exchange efficiency at the electrode surface than that of polymer **3a** above 20 mV/s.[21] Consequently, polymer **3b** has always a smaller peak separation ΔE but larger $|i_p|$ values than **3a** at the same scan rate v, especially at higher scan rates. That is to say, the electrode process of PFS polymers with lower content of coumarin moieties would become less reversible with increasing scan rate. It is worth noting that the αn_αvalue of polymer **3b** is reduced from 1.45 to 0.52 after photodimerization for 180 min and the K_s value is largely reduced also. This implies that the electrode process of the cross-linked polymer **3b** become less reversible. Because the whole-substituted **3b*** forms a denser film resulting from a higher cross-linking density, the rate of the electrolyte diffusion and electron exchange efficiency at the electrode surface are significantly reduced. As a result, polymer **3b** has much smaller peak separation ΔE but larger $|i_p|$ values than **3b*** at the same v over the range of 20 mV/s. Another possible reason may be that the dimerization of the coumarin moiety weakens its electron-donating capability. As for the half-substituted **3a**, UV irradiation does not lead to a significant change of αn_α and K_s, but reduces its D_{app} value; this may be due to a low cross-linking density in the film of **3a***. Hence, the electrochemical reversibility of polymers **3** decreases with increasing scan rate in the order of **3b**, **3a**, **3a***, and **3b***.

The CV results have demonstrated that the electrochemical process is diffusion controlled and quasireversible in a certain

Table 2. Relationships between the Peak Separation (ΔE), the Peak Current (i_p), and the Scan Rate (v), along with the Kinetic Parameters, αn_α, k_s, and D_{app} Obtained for the Polymer-Modified Electrodes

polymers	equations	r	$C_0^* \times 10^3$ (mol/cm^3)	αn_α	$k_s \times 10^8$ (cm^2/s)	$D_{app} \times 10^{12}$ (cm/s)
3a	ΔE (V) = 0.3777 + 0.1358 log v	0.9983				
	i_{pa} (μA) = 4.550 + 51.76 $v^{1/2}$	0.9936	3.319	0.43	2.43	1.20
	i_{pc} (μA) = 0.0939 − 71.66 $v^{1/2}$	−0.9960			4.66	2.29
3b	ΔE (V) = 0.2055 + 0.0407 log v	0.9978				
	i_{pa} (μA) = 16.44 + 186.9 $v^{1/2}$	0.9963	3.451	1.45	6700	5.01
	i_{pc} (μA) = 16.50 − 158.4 $v^{1/2}$	−0.9988			4810	3.60
3a*[a]	ΔE (V) = 0.4057 + 0.1282 log v	0.9996				
	i_{pa} (μA) = 7.141 + 16.43 $v^{1/2}$	0.9974	3.319	0.46	0.63	0.113
	i_{pc} (μA) = 0.088 − 41.91 $v^{1/2}$	−0.9907			4.10	0.735
3b*[a]	ΔE (V) = 0.4600 + 0.1145 log v	0.9959				
	i_{pa} (μA) = 8.035 + 138.6 $v^{1/2}$	0.9995	3.451	0.52	374	7.68
	i_{pc} (μA) = 14.49 − 124.5 $v^{1/2}$	−0.9987			302	6.19

[a] After UV irradiation for 180 min

scan rate range. The difference in coumarin content and different cross-linking density after photodimerization of coumarin uniting has a significant effect on the electrochemical behavior of the polymers **3** taking into account the change of kinetic parameters, αn_α, K_s, and D_{app}.

4. Conclusions

Novel photoreversible poly(ferrocenylsilanes) with different coumarin contents are synthesized by introducing 7-hydroxycoumarin into PFS side chain via macromolecular nucleophilic substitution reactions. These photoreversible PFS polymers exhibit interesting photochemical reactivity and electrochemical behavior. This study demonstrate that the content of coumarin substitutes on silicon have a significant effect on the photochemical and electrochemical behaviors of photoreversible PFS polymers. The whole-substituted polymer exhibits a higher degree of photodimerization and photoscission than the half-substituted one, but the latter has less reversible redox activity than the former in high scan rate range. It is interesting that the photodimerization and photoscission reactions also significantly affect the electrochemical behavior of the two PFS polymers. The electrochemical behavior of the two polymers almost reversibly changes with photodimerization and photoscission, but the photodimerization leads to a lower reversibility of electrode processes of the two polymers due to the slow rate of the electrolyte diffusion and charge transfer and low electron exchange efficiency resulting from the cross-linking of the films. Hence, these new photoreversible poly(ferrocenylsilanes) may have potential use as photomemory materials, redox-active gels, redox drug controlled-releasing carriers, and redox switching of optical properties because they combine the useful photchemical property with redox activity.

Acknowledgment. We thank the reviewers for their valuable comments, which greatly improved the quality of the manuscript. The financial support from the NSF of China (20374021, 50673029, and 20534020), the NSF of Guangdong Province (05006561), and the Program for New Century Excellent Talents in University are gratefully acknowledged.

Supporting Information Available: Methods of synthesis of poly(ferrocenyl(3-chloropropyl)methylsilane) and poly(ferrocenyl-(3-iodopropyl)methylsilane). NMR spectra of **2**, **3a**, and **3b**. TG thermograms and DSC curves of polymers **3**. This material is available free of charge via the Internet at http://pubs.acs.org.

References and Notes

(1) Turner, M. L. *Annu. Rep. Prog. Chem., Sect. A* **2000**, *96*, 491.
(2) (a) Manners, I. *Science*, **2001**, *294*, 1664. (b) Manners, I. *J. Polym. Sci., Part A: Polym. Chem.* **2002**, *40*, 179.
(3) Foucher, D. A.; Tang, B. Z.; Manners, I. *J. Am. Chem. Soc.* **1992**, *114*, 6246.
(4) Kulbaba, K.; Manners, I. *Macromol. Rapid Commun.* **2001**, *22*, 711.
(5) (a) Rulkens, R.; Ni, Y.; Manners, I. *J. Am. Chem. Soc.* **1994**, *116*, 12121. (b) Wang, X.-S.; Winnik, M. A.; Manners, I. *Macromol. Rapid Commun.* **2002**, *23*, 210. (c) Kim, K. T.; Vandermeulen, G. W. M.; Winnik, M. A.; Manners, I. *Macromolecules* **2005**, *38*, 4958.
(6) (a) Nguyen, M. T.; Diaz, A. F. *Chem. Mater.* **1994**, *6*, 952. (b) Manners, I. *Adv. Organomet. Chem.* **1995**, *37*, 131.
(7) (a) Korczagin, I.; Golze, S.; Hempenius, M. A.; Vancso, G. J. *Chem. Mater.* **2003**, *15*, 3663. (b) Kulbaba, K.; Resendes, R.; Cheng, A.; Bartole, A.; Safa-Sefat, A.; Coombs, N.; Stöver, H. D. H.; Greedan, J. E.; Ozin, G. A.; Manners, I. *Adv. Mater.* **2001**, *13*, 732. (c) Power-Billard, K. N.; Manners, I. *Macromolecules* **2000**, *33*, 26. (d) Kulbaba, K.; MacLachlan, M. J.; Evans, C. E. B.; Manners, I. *Macromol. Chem. Phys.* **2001**, *202*, 1768. (e) Gómez-Elipe, P.; Resendes, R.; Meadonald, P. M.; Manners, I. *J. Am. Chem. Soc.* **1998**, *120*, 8348. (f) Kulbaba, K.; Cheng, A.; Bartole, A.; Greenberg, S.; Resendes, R.; Coombs, N.; Safa-Sefat, A.; Greedan, J. E.; Stöver, H. D. H.; Ozin, G. A.; Manners, I. *J. Am. Chem. Soc.* **2002**, *124*, 12524. (g) Lammertink, R. G. H.; Hempenius, M. A.; Chan, V. Z.-H.; Thomas, E. L.; Vancso, G. J. *Chem. Mater.* **2001**, *13*, 429.
(8) Tang, H.; Liu, Y.; Chen, X.; Qin, J.; Inokuchi, M.; Kinoshita, M.; Jin, X.; Wang, Z.; Xu, B. *Macromolecules* **2004**, *37*, 9785.
(9) (a) Zechel, D. L.; Hultzsch, K. C.; Rulkens, R.; Balaishis, D.; Ni, Y.; Pudelski, J. K.; Lough, A. J.; Manners, I. *Organometallics* **1996**, *15*, 1972. (b) Power-Billard, K. N.; Manners, I. *Macromolecules*, **2000**, *33*, 26. (c) Wang, Z.; Manners, I. *Macromolecules* **2002**, *35*, 7669.
(10) Liu, X.; Bruce, D. W.; Manners, I. *J. Organomet. Chem.* **1997**, *548*, 49−56.
(11) Hempenius, M. A.; Robins, N. S.; Lammertink, R. G. H.; Vancso, G. J. *Macromol. Rapid Commun.* **2001**, *22*, 30.
(12) (a) Hempenius, M. A.; Vancso. G. J. *Macromolecules* **2002**, *35*, 2445. (b) Hempenius. M. A.; Brito, F. F.; Vancso. G. J. *Macromolecules* **2003**, *36*, 6683.
(13) Hempenius, M. A.; Péter, M.; Robins, N. S.; Kooij, E. S.; Vancso, G. J. *Langmuir* **2002**, *18*, 7629.
(14) Cyr, P. W.; Rider, D. A.; Kulbaba, K.; Manners, I. *Macromolecules* **2004**, *37*, 3959.
(15) Trenor, S. R.; Shultz, A. R.; Love, B. J.; Long, T. E. *Chem. Rev.* **2004**, *104*, 3059.
(16) Zhao, D.; Ren, B.; Liu, S.; Liu, X.; Tong, Z. *Chem. Commun.* **2006**, 779.
(17) Manners, I. *Chem. Commun.* **1999**, 857.
(18) Obi, M.; Morino, S.; Ichimura, K. *Chem. Mater.* **1999**, *11*, 656.
(19) Lee, S. W.; Kim, S. I.; Lee, B.; Kim, H. C.; Chang, T.; Ree, M. *Langmuir* **2003**, *19*, 10381.
(20) Bard, J.; Faulkner, L. R. *Electrochemical Methods*; John Wiley & Sons: New York, 1980; Chapter 6.
(21) Wang, X.; Wang, L.; Wang, J.; Chen, T. *J. Phys. Chem. B* **2004**, *108*, 5627; Laviron, E. *J. Electroanal. Chem.* **1979**, *101*, 19; Laviron, E.; Roulier, R. *J. Electroanal. Chem.* **1980**, *115*, 65; Deng, X.-H.; Kan, X.-W.; Yu, Y.; Zhang, W.-Z.; Liu, H.-Y.; Fang, B. *Acta Phys.-Chim. Sin.* **2005**, *21*, 1399.

MA062502O